Deliverable 7.8

D7.8 Report on first results of ground-motion testing

Deliverable information	
Work package	[WP 7: Testing: Rigorous testing and validation of dynamic risk components]
Lead	[GFZ]
Authors	[Karina Loviknes (GFZ), Danijel Schorlemmer (GFZ), Graeme Weatherill (GFZ), Tara Evaz Zadeh (GFZ), Fabrice Cotton (GFZ)]
Reviewers	[Management Board]
Approval	[Management Board]
Status	[Draft]
Dissemination level	[Public]
Will the data supporting this document be made open access? (Y/N)	N/A
If No Open Access, provide reasons	
Delivery deadline	[28.02.2023]
Submission date	[28.02.2023]
Intranet path	[DOCUMENTS/DELIVERABLES/]

Summary

As already reported in Deliverable D7.5, this deliverable has been hampered strongly by the canceled deployment of low-cost sensors (due to the international chip crisis) in the test areas as were planned in the proposal. For the investigation of high-resolution ground-motion models (GMM), an experiment in the Valais, Switzerland, area was planned in order to cover the sedimentary basin and the mountain slopes on each side of the valley with instruments. Measurement in such an environment would have provide the necessary high-resolution recordings for the envisioned study. To compensate for that, we teamed up with the URBASIS project (see Acknowledgments) and conducted a study on non-linear GMMs to investigate whether or not the concept of non-linearity is warranted by the data and we also investigated the impact of local geology on earthquake ground motions.

Likewise, due to a lack of distributed low-cost sensors in buildings in Europe, we were not able to develop the necessary testing metrics for exposure/risk testing as no measurements were available. However, to compensate for this, we have collected damage reports of the 29 December 2020 M6.4 Petrinja earthquake and the 6 February 2023 M7.8 Turkey-Syria earthquake sequence. The building-scale exposure model from task T2.7 has been finished (Deliverable D2.13) and we provide first tests of the exposure model (in combination with the respective fragility model) against real damage assessments.

Testing of nonlinear site-amplification models

Introduction

Nonlinear site effects mainly occur for large ground motion at soft soils where there are few measured observations. Predicting and modeling such effects is therefore challenging, and most nonlinear site amplification models used in ground-motion models (GMMs) are either partly or fully based on numerical simulations. To test the prediction power of nonlinear site-amplification models, Loviknes et al. (2021) developed a testing framework using observed site-amplification from the KiK-net network in Japan. In this report we summaries the method of Loviknes et al. (2021) and show an example using the software codes given in D7.4 (see above).

The Japanese Kiban-Kyoshin network (KiK-net) is a part of the National Research Institute for Earth Science and Disaster Prevention (NIED), and one of the most comprehensive strong-motion networks in the world (Aoi et al. (2011)). The KiK-net network have been recording since 1996 and consist of 692 stations with instruments in both borehole and at the ground surface. Several of the KiK-net stations have recorded earthquakes in a wide range of ground motion intensity, including high intensity ground motions with the potential to trigger nonlinear site amplification (Régnier et al., 2013). The KiK-net network is therefore ideal for testing nonlinear site-amplification prediction models.

Method

The testing framework of Loviknes et al. (2021) consist of three parts:

1. A simple linear ground-motion model is derived on the dataset of interest.
2. The residuals between the predicted linear ground motion and each observation are split into between-event, between-site random effect and record-to-record variability.
3. Site-amplification models are tested against the residuals of individual well-recorded stations and stations grouped into site proxy bins.

Each step is described in further details in the following sections.

The aim of the two first steps in the method of Loviknes et al. (2021) is to obtain the observed site amplification. First the linear site amplification is derived using a linear GMM. The linear GMM is derived using only the linear part of the dataset, that is, small ground motions below a certain threshold or ground motions recorded on hard rock sites. Loviknes et al. (2021) sets the peak ground acceleration (PGA) threshold to PGA = 0.05g following Régnier et al. (2013) and the V_{S30} (time-averaged shear-wave velocity in the upper 30m of a 1-D soil column) threshold for rock sites to V_{S30} = 760m/s. The linear GMM of Loviknes et al. (2021) is developed following the same method and functional form as the GMM by Kotha et al. (2018):

$$\ln(\mathrm{PSA}) = f_R(M_W,R_{JB}) + f_M(M_W) + \delta B_e + \delta S2S_s + \delta WS_{e,s} \qquad (1)$$

With fixed effects $f_R(M_W,R_{JB})$ and $f_M(M_W)$ capturing the scaling of pseudo spectral acceleration (PSA) with distance and magnitude, and random effects δB_e and $\delta S2S_s$ quantifying the event and site variability, respectively. $\delta WS_{e,s}$ is the record-to-record variability. The model does not include a fixed-effect site term based on V_{S30}, and the $\delta S2S_s$ therefore captures all site-specific response and can be used as the empirical site-amplification function (Kotha et al., 2018).

Secondly, the prediction of the linear GMM $\mu_{e,s}$ for an event e and site s is subtracted from the corresponding observed ground motion $Y_{e,s}$, to obtain the total residual $\epsilon_{e,s}$:

$$\epsilon_{e,s} = \ln Y_{e,s} - \ln \mu_{e,s} \qquad (2)$$

The total residual $\epsilon_{e,s}$ is then split to quantify the random effects of the events and sites into the event and site variability:

$$\epsilon_{e,s} = \delta B_e + \delta S2S_s + \delta WS_{e,s} \qquad (3)$$

Here δB_e and $\delta S2S_s$ are the event and site term representing the systematic deviation between the observed ground motions, from the median predictions of the GMM, and $\delta WS_{e,s}$ is the "left-over" residual capturing the record-to-record variability.

Both the GMM development and the splitting of the residuals are performed using the mixed-effects regression algorithm *lmer* by Bates et al. (2015) in the statistical program R. A mixed effects regression model includes both fixed-effect (explanatory variables) and random-effect terms (grouping factors) in the regression to deal with hierarchical data (Bates et al., 2015). The predicted response spectra and aleatory variability of the linear GMMs at 50 km R_{JB} distance for different magnitudes are shown in Figure 1.

To evaluate how well the derived GMM scales with magnitude and distance, a residual analysis should be performed. Figure 2 and 3 show the distributions of δB_e with respect to magnitude, $\delta S2S_s$ with respect to V_{S30}, and $\delta WS_{e,s}$ with respect to distance for the linear GMMs and the split residuals, respectively. In both figures, δB_e with magnitude and $\delta WS_{e,s}$ with distance have a mean consistently close to zero and no clear trend. This confirms that the scaling with magnitude and distance are well captured. For $\delta S2S_s$ a down-going trend with V_{S30} is observed, this is however expected because a V_{S30} site term was not included in the fixed effects (Kotha et al., 2018).

The final step of the testing procedure is to evaluate the prediction power of non-linear site-

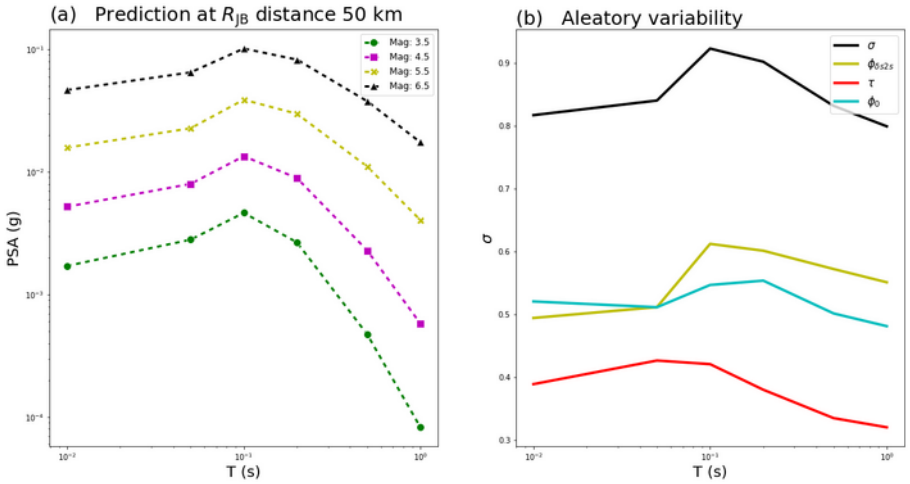

Figure 1: (a) Response spectra of pseudo spectral acceleration (PSA) for different magnitudes at R_{JB} 50 km, and (b) the total aleatory variability σ and standard deviations τ, φs2s and φ0.

amplification models compared to the prediction power of a linear site amplification model. Because the "left-over" residual $\delta WS_{e,s}$ is expected to contain the non-linear site response, the linear site-amplification model is defined as $\delta WS_{e,s} = 0$ for every value of $PGA_{rock} \exp(\delta B_e)$. The models are tested on the site response of individual soft-soil stations ($V_{S30} < 760$ m/s) that have recorded at least 4 records with PGA > 0.05g.

The prediction power of the amplification models is measured in mean absolute error (MAE):

$$MAE_S = \frac{|\sum_{e}^{N} \delta WS_{e,s} - F_{e,s}|}{N} \qquad (6)$$

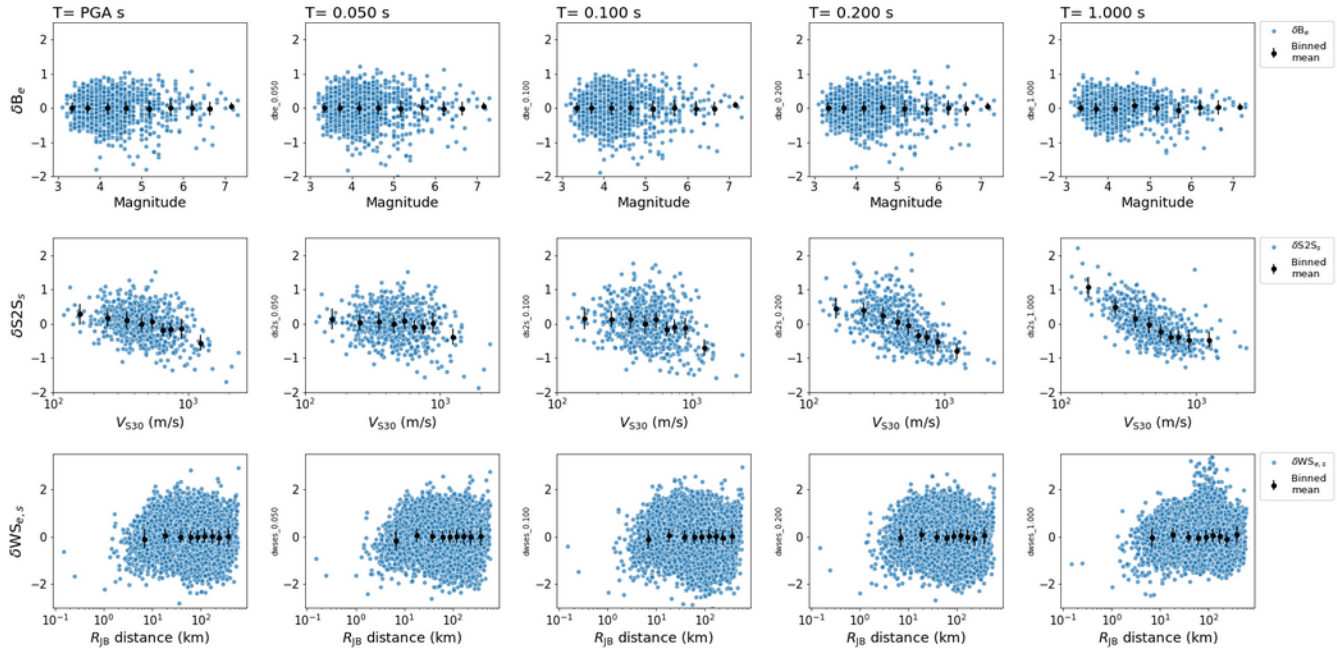

Figure 2: Random effect residual plot from the mixed-effect regression used to develop the linear ground-motion model. (Top row, a–d) Distribution and binned mean of δBe with magnitude for each period T. (Center row, e–h) Distribution and binned mean of δS2Ss with VS30 in log-scale for each period T. (Bottom row, i–l) Distribution and binned mean of δWSe,s with R_{JB} distance. The binned means are with 95% confidence interval. The means of δBe and δWSe,s has a mean centered around zero and do not show any trend with magnitude and distance, this show that the GMM regression has captured the scaling of magnitude and distance, while δS2Ss shows a negative trend with V_{S30} because a V_{S30} site-term was not included in the fixed effects (Equation 1).

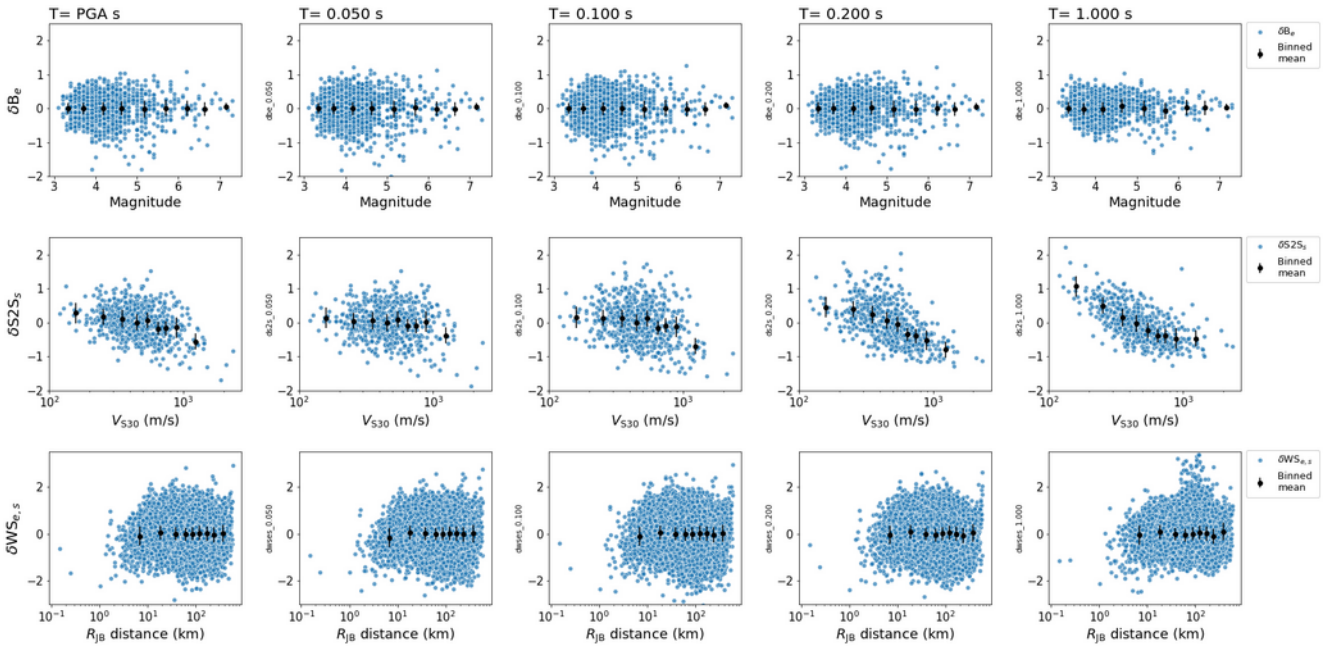

Figure 3: Random effect residual plot as in Figure 2. Here the residuals are from the splitting of the total residual (Equation 2) using mixed-effect regression.

here $F_{e,s}$ is the modeled site-amplification and MAE_s is the mean absolute error for each site s for N number of events e. For each site and period the model with the lowest score is considered the best model. However, it is important to note that the MAE score only measures the deviation between the residuals and the predictions of the amplification models and does not have direct physical meaning. The model is therefore only best in a relative sense (Mak et al., 2015).

Models and Dataset

Loviknes et al. (2021) tested the non-linear site-amplification models of Seyhan and Stewart (2014), Sandikkaya et al. (2013), Hashash et al. (2020) and the site-amplification model in the GMM of Abrahamson et al. (2014). In this report, for simplicity, we only test the site amplification models of Seyhan and Stewart (2014) (SS14) and Abrahamson et al. (2014) (ASK14). Both these models were developed as a part of the NGA-West2 project and based on the simulations of Kamai et al. (2014).

We test the models against site amplification derived from ground motion records recorded by KiK-net stations and processed and compiled into a dataset by Bahrampouri et al. (2020). We only use onshore events with depth ≤ 35km, recorded at R_{JB} < 600km, with the recommended usable frequency bandwidth of at least 60% of the range from zero to the Nyquist frequency (Bahrampouri et al., 2020).

Results

Out of all the soft-soil stations in the KiK-net network, 19 stations have recorded sufficient strong-motion records to be included in the test, the locations of these stations are shown in Figure 4. For most of the selected stations, the linear site amplification model had the best score (blue triangles in Figure 4). Only 5 stations had a nonlinear site amplification model score better than the linear amplification model (red triangles in Figure 4). Figure 5 shows the site response of one of the stations selected for the test. For this station, IBRH12, the two non-linear amplification models has the best score for most of the periods and a slight down-going trend between $\delta\text{WS}_{e,s}$ and PGA is observed. However, for most of the KiK-net stations, the observed site response shows a large variability and little clear trend, even within stations with similar V_{S30} values. This is especially clear when the stations are grouped by V_{S30} as

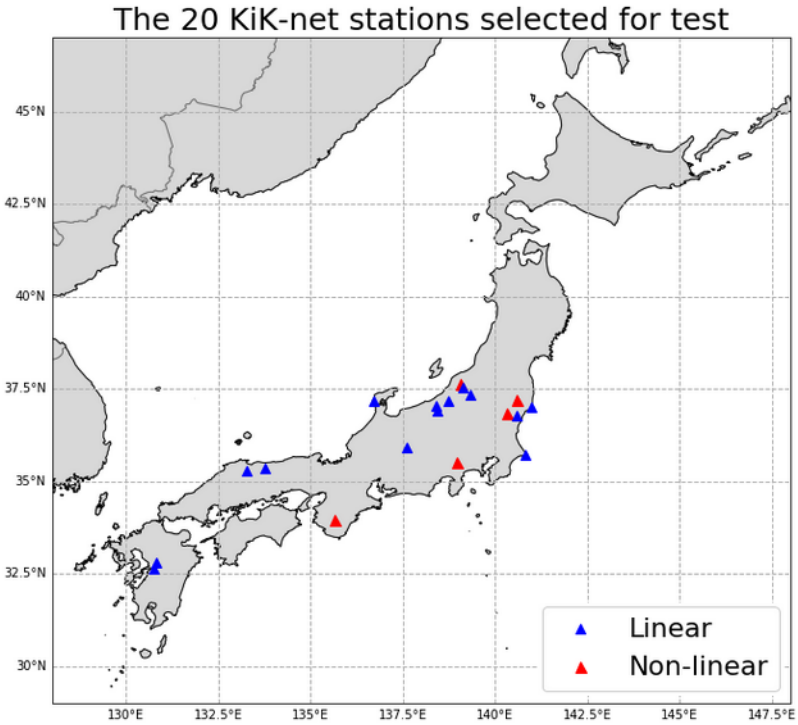

Figure 4: Map of Japan showing the location of the stations selected for the test. The blue triangles show the stations where the linear amplification model had the best score, and the red triangles show the stations where one of the non-linear amplification models had the best score.

in Figure 6.

Discussion and conclusion

This report summarizes the method of the testing framework of Loviknes et al. (2021) for testing nonlinear site amplification model used in ground motion models. The method uses mixed-effects regression to derive a linear GMM and split the residuals between the observation and linear predictions into event, site and record-to-record variability. The residuals are then used to test nonlinear

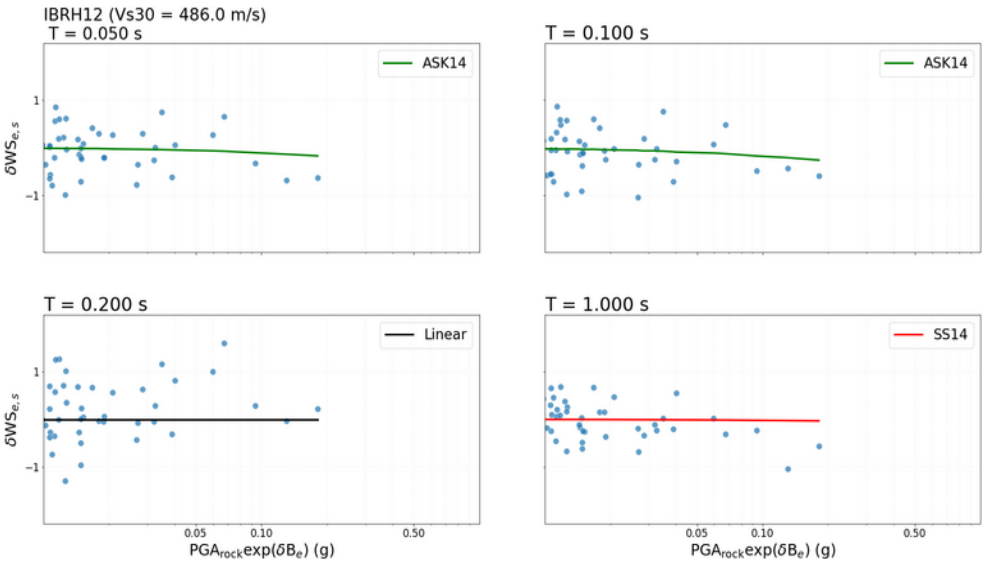

Figure 5: Station IBRH12 with the best linear and non-linear site amplification models of each period, compared to δWSe,s with respect to rock peak acceleration with event variability (PGA_{rock} exp(δBe)). The non-linear models are from Seyhan and Stewart (2014) (SS14) and Abrahamson et al. (2014) (ASK14).

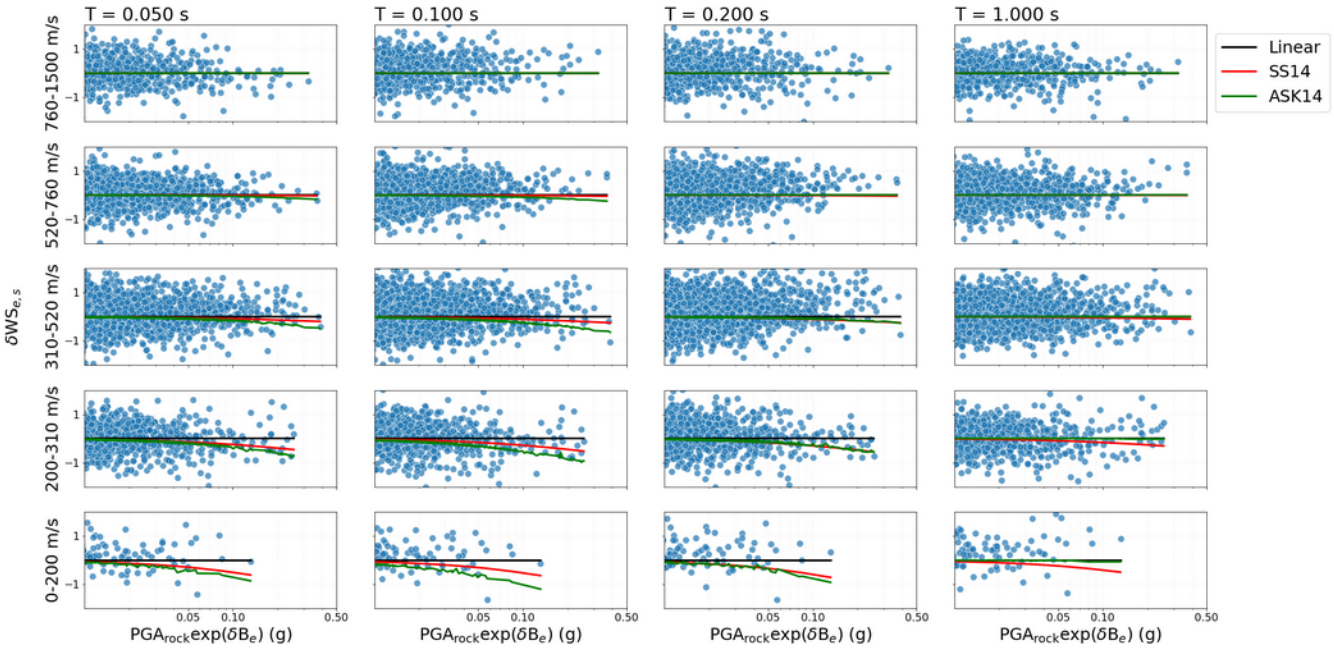

Figure 6: The KiK-net stations grouped by V_{S30} with the linear and non-linear site amplification models compared to δWSe,s with respect to rock peak acceleration with event variability (PGA_{rock} exp(δBe)). The non-linear models are from Seyhan and Stewart (2014) (SS14) and Abrahamson et al. (2014) (ASK14). The trend predicted by the models are not observed.

site-amplification models against a linear site-amplification model. Loviknes et al. (2021) found that, for most stations, the simple linear site amplification model has the best performance. Loviknes et al. (2021) considered ground motions up to 0.2 g, and therefore argues that using nonlinear site-amplification models in this ground-motion range is not necessary. The study only considers nonlinear amplification models based on V_{S30} and PGA, other models using other parameters to capture non-linearity should therefore be tested in the future.

The main limitations of the test is the limited number of strong ground-motions. For Japan adding records from the Knet network to the test, is in planning. For Italy and California, Loviknes et al. (2022) applied the same test using the ESM (Luzi et al. 2016, Lanzano et al., 2021) and NGA-West2 (Ancheta et al., 2014) datatsets, respectively. Loviknes et al. (2022) found that for both Italy and California, the within-station site-response variability was smaller than for Japan and the nonlinear site-amplification models had an overall better performance. However, the number of strong ground-motions are still limited and the nonlinear amplification models are not able to capture the non-linearity at high V_{S30} > 500 m/s. Alternative site proxies used to characteristic non-linear site amplification should therefore be investigated in future studies.

Testing a new site proxy for site-amplification prediction models

Local geology can have a strong impact on earthquake ground shaking. This is especially true for sites with mainly loose sediments which are expected to amplify the recorded ground motion. In many, non-site-specific, applications where seismic hazard and risk assessments must be computed on large regions, this site amplification is commonly predicted using the average shear-wave velocity of the upper 30 meters of the soil column (VS30). For a single site, the velocity profile and VS30 can be measured directly, but for larger areas and regions the VS30 must be inferred from other parameters. A much-used method to calculate VS30 is the model by Wald and Allen (2007) based on topographic slope from digital elevation models (DEMs). However, inferring VS30 based on topographic slope has several limitations, especially for basins and particular geological conditions (Lemoine et al. 2012). Furthermore, the measured VS30 values should not be used interchangeably with inferred VS30 values

without properly accounting for the additional uncertainty related to the VS30 calculations (Lemoine et al. 2012, Weatherill et al. 2020).

In this study we propose a geomorphological model for inferred sediment depth by Pelletier et al. (2016), as an alternative site proxy to predict ground motion site-amplification on a regional or global scale. The Pelletier et al. (2016) model use DEM and geological maps to distinguish between lowlands, uplands, hill slopes and valley bottoms. The thickness of sediments, soil and intact regolith is then inferred for each landform using several global and regional parameters from geological maps, water table depth and climate data. The final model provides a global map of inferred regolith, soil and sediment thickness up to 50 meters as in Pelletier et al. (2016). In this study we focus on the average soil and sediment thickness, from hereon called geomorphologically-inferred sedimentary thickness, as shown in Figure 7 for Europe.

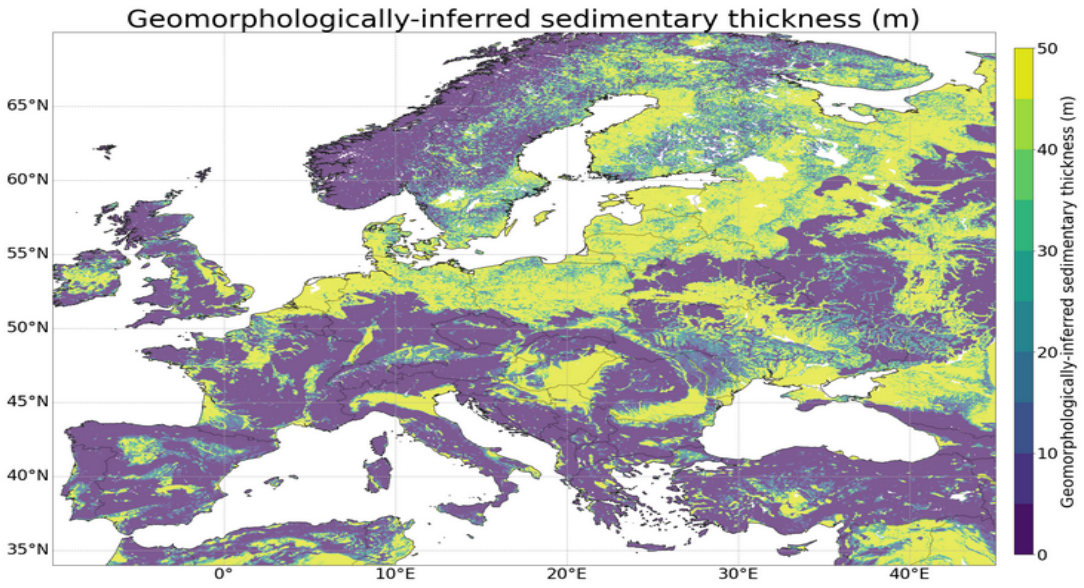

Figure 7: The inferred geomorphologically-inferred sedimentary thickness for Europe from the Pelletier et al. (2016) model.

To test whether the model can be used to predict ground-motion site amplification, we compare the geomorphologically-inferred sedimentary thickness to inferred V_{S30}, topographic slope and empirical site amplification as shown in Figure 8 for frequency $f = 1.062$ Hz. The empirical site amplification is derived as the site-to-site residuals ($\delta S2S_s$) derived from a simple GMM following the method of Kotha et al. (2020) and using the European Engineering Strong-Motion (ESM) dataset (Luzi et al., 2020). For each proxy we use linear regression to derive a simple site amplification model (black lines in Figure 8) and evaluate the performance of each model. The results show that the geomorphologically-inferred sedimentary thickness performs better than or equally well as the traditional and much used proxies V_{S30} inferred from topographic slope and topographic slope. We therefore argue that the inferred geomorphologically-inferred sedimentary thickness from the Pelletier et al. (2016) model is a promising new alternative to traditional inferred proxies for predicting site amplification on a regional or global level for large scale seismic hazard or risk studies.

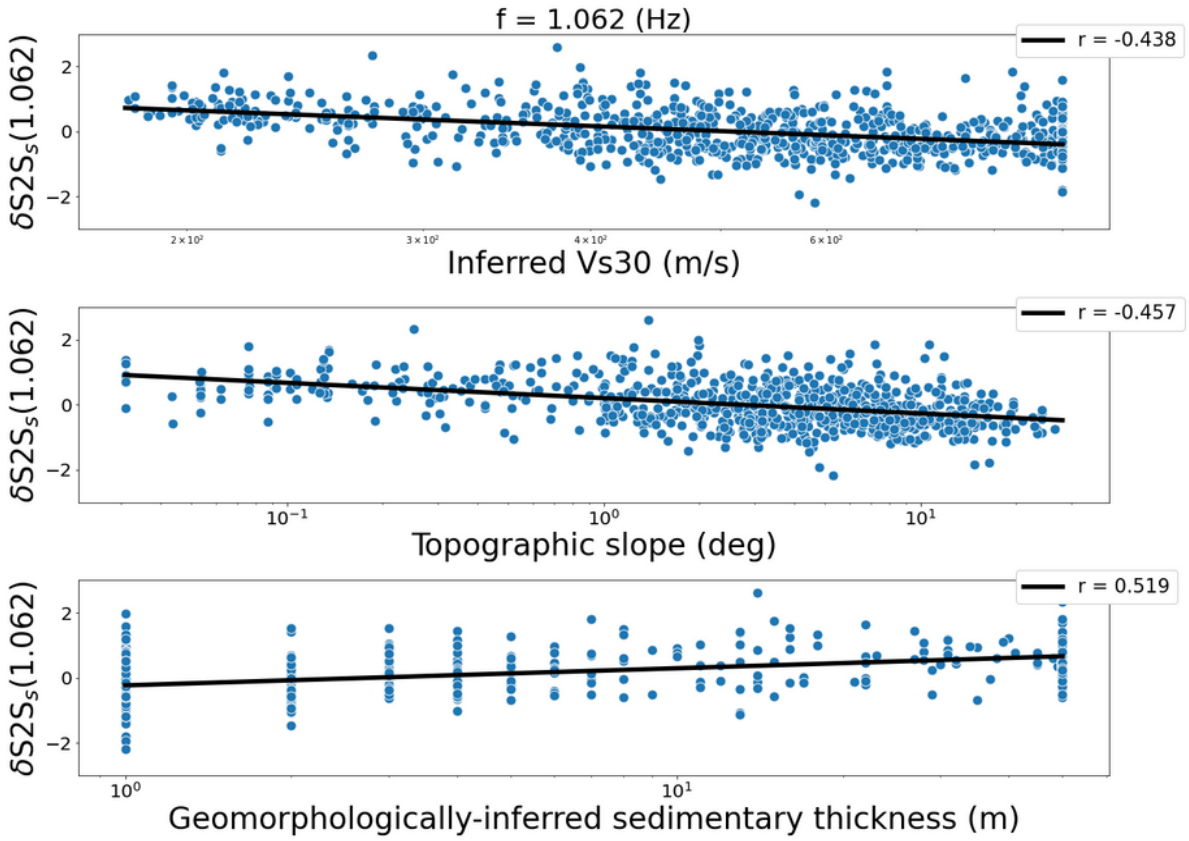

Figure 8: The linear regression (black lines) and correlation coefficient r between the empirical site amplification δS2Ss for frequency f=1.062 Hz and the inferred V_{S30} from topographic slope (top) and topographic slope (middle) and the geomorphologically-inferred sedimentary thickness (bottom) at stations from the European Engineering Strong-Motion (ESM) dataset.

Preliminary Testing of Damage and Loss Assessments

We have tested the scenario risk assessment for the Turkey 2023 and Petrinja 2020 earthquakes. For this, we have used excerpts of the Global Dynamic Exposure model (Deliverable D2.13) for the affected areas. Although this deliverable only covers the model for European countries, we have extended it to cover Syria as it was also heavily impacted by the earthquake. This was done by including the Middle East exposure model provided by the Global Earthquake Model.

To separately check for damage and loss, we have developed the loss-calculator (see Deliverable D2.13) that aggregates damage and loss to either buildings or tiles of a grid. To compute the damage and loss of the earthquakes, we use the most recent ShakeMap provided by the United States Geological Survey (USGS) for the Turkey[1] and Petrinja[2] earthquakes.

Turkey Earthquake

Our results show a good match between the building-specific assessment of damage and the true

1https://earthquake.usgs.gov/earthquakes/eventpage/us6000jllz/executive
2https://earthquake.usgs.gov/earthquakes/eventpage/us6000d3zh/executive

numbers as reported in the media. 164,000 completely or severely damaged buildings were reported (including some that collapsed during the aftershocks) and the model was able to reproduce a similar number: 96,000 completely collapsed and 38,000 extensively damaged buildings, totaling to 144,000 completely or severely damaged buildings. The difference is little more than 10% of the total number including the results of the aftershock damage. This indicates that at least the combination of exposure data and fragility functions shows an agreement with the observations. Contrary to that, the number of fatalities is computed at 8,300 and significantly lower than the recently reported more than 50,000 casualties. This points to two possible problems: either the vulnerability functions are not well calibrated or the number of people considered inside of buildings are wrongly estimated in the exposure model. Such functions or numbers are difficult to estimate and also the USGS reports[3] with almost equal probability fatalities ranging from 1,000 to 1,000,000, indicating that our results are within the same range. Finding the true cause of this mismatch will continue after the RISE project as will the further development of the exposure model form Deliverable D2.13.

Petrinja, Croatia Earthquake

For the Petrinja earthquake the model prediction were significantly above the observed numbers. Using the ShakeMap from the USGS, our model predicts 31,500 collapsed and 13,500 extensively damaged buildings while only 4,200 buildings were reported as uninhabitable and approx. 8000 temporarily uninhabitable. Likewise the number of fatalities is predicted to be around 700 while only 8 people were reported dead. This mismatch requires a more in-depth study to identify the problem.

Acknowledgments

The authors are grateful to Bahrampouri et al. (2020) for their open-source dataset and to Jean Braun for valuable discussion and explanation on regolith. In addition, the authors would like to thank the open-source community for the Linux operating system and the many programs used in this study. Karina Loviknes is funded by the European Commission, ITN Marie Sklodowska-Curie URBASIS-EU project, under the grant agreement 813137, Danijel Schorlemmer is funded by the European Union's Horizon 2020 research and innovation program Real-time Earthquake Risk Reduction for a Resilient Europe "RISE" project, under grant Agreement 821115.

References

Abrahamson, N. A., Silva, W. J., and Kamai, R. (2014). "Summary of the ASK14 ground motion relation for active crustal regions". *Earthquake Spectra*, **30**(3):1025–1055.

Aoi, S., T. Kunugi, and H. Fujiwara (2004). Strong-motion seismograph network operated by NIED: K-NET and KiK-net, J. Japan Assoc. Earthq. Eng. 4, 65–74.

Ancheta, T. D., Darragh, R. B., Stewart, J. P., Seyhan, E., Silva, W. J., Chiou, B. S., Wooddell, K. E., Graves, R. W., Kottke, A. R., Boore, D. M., Kishida, T., and Donahue, J. L. (2014). "NGA-West2 database". *Earthquake Spectra*, **30**(3):989–1005.

Bahrampouri, M., Rodriguez-Marek, A., Shahi, S., and Dawood, H. (2020). "An updated database for ground motion parameters for KiK-net records". *Earthquake Spectra*, page 875529302095244.

Bates, D., Mächler, M., Bolker, B. M., and Walker, S. C. (2015). "Fitting linear mixed-effects models

3https://earthquake.usgs.gov/earthquakes/eventpage/us6000jllz/pager

using lme4." *Journal of Statistical Software*, **67**(1).

Hashash, Y. M., Ilhan, O., Hassani, B., Atkinson, G. M., Harmon, J., and Shao, H. (2020). "Significance of site natural period effects for linear site amplification in central and eastern North America: Empirical and simulation-based models." *Earthquake Spectra*, **36**(1):87–110.

Kamai, R., Abrahamson, N. A., and Silva, W. J. (2014). "Nonlinear horizontal site amplification for constraining the NGA-West2 GMPEs." *Earthquake Spectra*, **30**(3):1223–1240.

Kotha, S. R., Cotton, F., and Bindi, D. (2018). "A new approach to site classification: Mixed-effects Ground Motion Prediction Equation with spectral clustering of site amplification functions." *Soil Dynamics and Earthquake Engineering*, 110:318–329.

Kotha, S.R., Weatherill, G., Bindi, D. and Cotton, F. (2020). A regionally-adaptable ground-motion model for shallow crustal earthquakes in Europe. *Bull Earthquake Eng* **18,** 4091–4125 doi:10.1007/s10518-020-00869-1

Lanzano, G., Luzi, L., Cauzzi, C., Bienkowski, J., Bindi, D., Clinton, J., Cocco, M., D'Amico, M., Douglas, J., Faenza, L. and Felicetta, C., 2021. Accessing European strong-motion data: An update on ORFEUS coordinated services. *Seismological Society of America*, *92*(3), pp.1642-1658.

Lemoine, A., Douglas, J., and Cotton, F. (2012); Testing the Applicability of Correlations between Topographic Slope and VS_{30} for Europe. *Bulletin of the Seismological Society of America* ; 102 (6): 2585–2599. doi:10.1785/0120110240

Luzi L., Puglia R., Russo E., D'Amico M., Felicetta C., Pacor F., Lanzano G., Çeken U., Clinton J., Costa G., Duni L., Farzanegan E., Gueguen P., Ionescu C., Kalogeras I., Özener H., Pesaresi D., Sleeman R., Strollo A., Zare M. (2016). The Engineering Strong-Motion Database: A Platform to Access Pan-European Accelerometric Data. Seismological Research Letters; 87 (4): 987–997.

Luzi L., Lanzano G., Felicetta C., D'Amico M. C., Russo E., Sgobba S., Pacor, F., and ORFEUS Working Group 5 (2020). Engineering Strong Motion Database (ESM) (Version 2.0). Istituto Nazionale di Geofisica e Vulcanologia (INGV). doi:10.13127/ESM.2

Loviknes, K., S. R. Kotha, F. Cotton, and D. Schorlemmer (2021). Testing Nonlinear Amplification Factors of Ground-Motion Models, Bull. Seismol. Soc. Am. 111, 2121–2137, doi: 10.1785/0120200386

Loviknes, K., F. Cotton, and D. Schorlemmer (2022). Testing of Site-Amplification Models used by Ground Motion Models. Deliverable 4.4: New challenges for Urban Engineering Seismology (URBASIS-EU), https://urbasis-eu.osug.fr/Scientific-Reports-157

Mak, S., Clements, R. A., and Schorlemmer, D. (2015). "Validating intensity prediction equations for Italy by observations." *Bulletin of the Seismological Society of America*, **105**(6):2942–2954

Pelletier, J. D., Broxton, P. D., Hazenberg, P., Zeng, X., Troch, P. A., Niu, G.-Y., Williams, Z., Brunke, M. A., and Gochis, D. (2016), A gridded global data set of soil, immobile regolith, and sedimentary deposit thicknesses for regional and global land surface modeling, *J. Adv. Model. Earth Syst.*, 8, 41– 65, doi:10.1002/2015MS000526.

Régnier, J., Cadet, H., Fabian Bonilla, L., Bertrand, E., and Semblat, J. F. (2013). “Assessing nonlinear behavior of soils in seismic site response: Statistical analysis on KiK-net strong-motion data.” *Bulletin of the Seismological Society of America*, **103**(3):1750–1770.

Sandikkaya, M. A., Akkar, S., and Bard, P. Y. (2013). “A nonlinear site amplification model for the next pan-European ground-motion prediction equations.” *Bulletin of the Seismological Society of America*, **103**(1):19–32.

Schorlemmer, D., Cotton, F., Delattre, F., Evaz Zadeh, T., Kriegerowski, M., Lingner, L., Oostwegel, L., Prehn, K., and Shinde, S. (2023). “D2.13 An open, dynamic, high-resolution exposure model for Europe” RISE Deliverable.

Seyhan, E. and Stewart, J. P. (2014). “Semi-empirical nonlinear site amplification from NGA-West2 data and simulations.” *Earthquake Spectra*, **30**(3):1241–1256.

Wald, D. J., Allen, T. I. (2007); Topographic Slope as a Proxy for Seismic Site Conditions and Amplification. *Bulletin of the Seismological Society of America*;; 97 (5): 1379–1395. doi:10.1785/0120060267

Weatherill G., Kotha S. R., and Cotton F. (2020) Re-thinking site amplification in regional seismic risk assessment. *Earthquake Spectra*., 36:274-297. doi:10.1177/8755293019899956